

# Across-horizon scattering and information transfer

V.A. Emelyanov\* and F.R. Klinkhamer†

*Institute for Theoretical Physics,  
Karlsruhe Institute of Technology (KIT),  
76128 Karlsruhe, Germany*

## Abstract

We address the question whether or not two electrically charged particles can Coulomb scatter if one of these particles is inside the Schwarzschild black-hole horizon and the other outside. It can be shown that the quantum process is consistent with the local energy-momentum conservation law. This result implies that across-horizon scattering is a physical effect, happening near astrophysical black holes. We propose a *Gedankenexperiment* which uses the quantum scattering process to transfer information from inside the black-hole horizon to outside.

Keywords: general relativity, black holes, quantum electrodynamics, Coulomb scattering

---

\* viacheslav.emelyanov@kit.edu

† frans.klinkhamer@kit.edu

## I. INTRODUCTION

Astrophysical black holes are expected to evaporate [1]. This quantum process leads to the information-loss problem in black-hole physics [2]. A final resolution of this problem could, as sometimes suggested, be based on principles that lie outside the framework of the standard semi-classical physics. But perhaps these nonstandard principles are not really needed, as the high-energy photon of quantum electrodynamics (QED) may be capable of propagating out of the black-hole horizon [3].

In this paper, we implement a particular approach to partial information recovery out of a black hole, without changing the principles of local quantum field theory. The main idea is based on the circumstance that a quantum field simultaneously exists at all spacetime points, including those of the region inside the black-hole horizon. Specifically, a quantum field is nonvanishing at each point of a given spacetime manifold and, according to the canonical (anti-)commutation relations, gives rise to random fluctuations of observables at each spacetime point, even in the vacuum state. A particle is a localized excitation, which significantly disturbs the quantum-field expectation value in its neighborhood. If the particle is sufficiently close to the black-hole horizon, the corresponding quantum-field disturbance is nontrivial even across the black-hole horizon. Since the quantum-field disturbance is not a quantity that must propagate at a particular speed (unlike real particles), this may cause the following across-horizon effect: two charged particles, located at different sides of the black-hole horizon, can scatter with each other via their quantum-field disturbances.

More concretely, the across-horizon-scattering effect can be understood as follows. In QED, the scattering interaction between charged particles at tree level (virtual-photon exchange) is mathematically described by the Feynman propagator  $G_F^{\mu\nu}(x, x')$  of the electromagnetic field (and, at higher orders in perturbation theory, also by the Feynman propagators of the electrically charged matter fields). This particular Green's function has a nonvanishing support for spacelike-separated points:  $G_F^{\mu\nu}(x, x') \neq 0$  holds even for two spacetime points with spacelike separation, whereas, for example, the retarded Green's function  $G_R^{\mu\nu}(x, x')$  vanishes identically for two spacetime points with spacelike separation. Hence, QED does not forbid the interaction between two electrically charged particles that are causally disconnected.

The crucial question, now, is if across-horizon scattering can be used to transfer information from the inside of the black-hole horizon to the outside. The present paper shows that, in practice, it may be difficult to use the across-horizon-scattering effect for information transfer but it is not impossible.

Throughout this article, we take  $c = G_N = \hbar = 1$ , unless otherwise stated. Gravity is assumed to be described by standard general relativity, based on the Einstein equivalence principle, and the metric signature is  $(+ - - -)$ . Interactions of elementary particles are taken to be described by standard quantum field theory over curved spacetime.

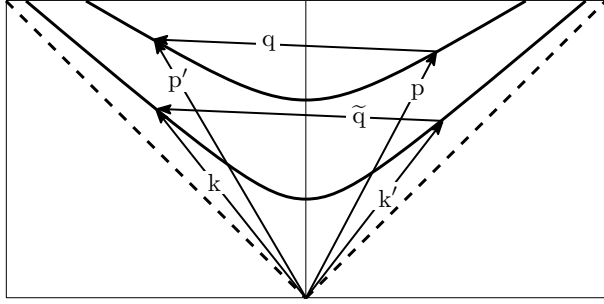


FIG. 1. Initial-particle momenta ( $p$  and  $k$ ) and final-particle momenta ( $p'$  and  $k'$ ), where the  $p$  and  $p'$  particles have a larger mass than the  $k$  and  $k'$  particles. Shown is a two-dimensional slice of the four-dimensional energy-momentum space, with energy along the vertical axis. The dashed line corresponds to the light-cone and all four particle momenta are timelike. Coulomb scattering (1) occurs if  $q \equiv p' - p$  equals  $\tilde{q} \equiv k - k'$ , which corresponds to energy-momentum conservation.

## II. SCATTERING

It appears that the Universe can be locally approximated by Minkowski spacetime. The Minkowski spacetime manifold is a fundamental ingredient of elementary particle physics for the description of high-energy interaction processes. In QED, the leading-order probability amplitude for the Coulomb scattering of two electrically charged particles (electron  $e^-$  and muon  $\mu^-$ ) is represented by the following tree-level Feynman diagram [4–6]:

$$\text{out}(\mu, p'; e, k' | \mu, p; e, k)_{\text{in}} \propto \text{Feynman Diagram} \quad (1)$$

The Feynman diagram shows two incoming particles,  $\mu, p'$  and  $e, k$ , represented by solid lines with arrows indicating the flow of negative electric charge and positive lepton number. They interact via a wavy line representing the Feynman photon propagator, which is a wavy line with arrows indicating the flow of positive electric charge and negative lepton number. The outgoing particles are  $\mu, p$  and  $e, k'$ , represented by solid lines with arrows indicating the flow of negative electric charge and positive lepton number.

with definition  $q \equiv p' - p$  and arrows showing the flow of negative electric charge (and also the flow of positive lepton number,  $L_\mu$  for the  $p$  particle and  $L_e$  for the  $k$  particle). The wavy line in the diagram on the right-hand-side of (1) stands for the Feynman photon propagator  $-ig_{\mu\nu}/(q^2+i\epsilon)$  with a positive infinitesimal  $\epsilon$ . The Feynman propagator, different from the retarded propagator, is a crucial ingredient for obtaining a unitary  $S$ -matrix (see, e.g., Sec. 3.7 and Chap. 8 of Ref. [5]). The amplitude (1) is identically zero, unless the energy-momentum conservation law is fulfilled,  $p + k = p' + k'$ .

In standard QED over Minkowski spacetime, the momenta of the particles before and after the Coulomb scattering are timelike four-vectors, whereas the momentum-exchange vectors  $q \equiv p' - p$  and  $\tilde{q} \equiv k - k'$  are spacelike four-vectors. Figure 1 gives a concrete example of these momenta, provided  $p'$  and  $k'$  satisfy the energy-momentum-conservation condition ( $q = \tilde{q}$ ).

Next, consider a neutral and nonrotating black hole of astrophysical size (mass  $M \gtrsim M_{\text{Sun}}$ ). In the region near the black-hole horizon, one can always introduce local Minkowski

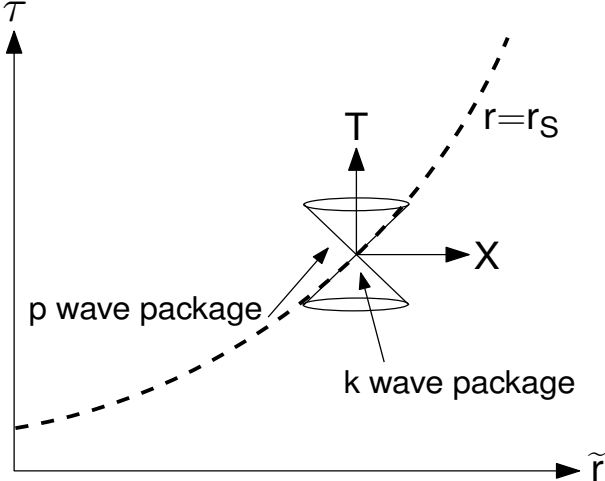


FIG. 2. In the vicinity of the black-hole horizon, coordinates can be chosen which are locally Minkowskian. A local inertial coordinate system (coordinates  $T, X, Y, Z$ ) can, for instance, be embedded in the  $(\tau, \tilde{r})$ -plane, where  $\tau$  and  $\tilde{r}$  are, respectively, Novikov's infalling-clock time coordinate and infalling-clock comoving radial coordinate [7]. With these local inertial coordinates ( $Y$  and  $Z$  pointing out of the plane shown), the figure sketches the light-cone in the neighborhood of the Schwarzschild horizon (dashed line) at standard radial coordinate  $r = r_S \equiv 2G_N M/c^2$ . In addition, the trajectories of two colliding wave packages are shown, one wave package with average momentum  $k$  is positioned outside the black-hole horizon and the other wave package with average momentum  $p$  is positioned inside the horizon. These momenta  $k$  and  $p$  correspond to those of the scattering process (1) and also appear in Fig. 1. For ultrarelativistic particles, the momenta  $k$  and  $p$  are close to their respective light-cones.

coordinates, according to the Einstein equivalence principle. For these local inertial coordinates  $(T, X, Y, Z)$ , part of the horizon of the black hole coincides locally with part of the light-cone shown in Fig. 2 (which is a simplified version of Fig. 3(a) in Ref. [7]). Locally, there is nothing in the inertial frame which marks the position of the projected horizon surface; see the second paragraph of App. A for further discussion. Figure 2 also shows the trajectories of two colliding wave packages, one outside the black-hole horizon with average momentum  $k$  and the other inside the horizon with average momentum  $p$ .

We are, now, ready to consider the collision of two electrically charged particles of different mass, where the muon with mass  $m_\mu$  is inside the black-hole horizon and the electron with mass  $m_e$  is outside. In a local inertial coordinate system (LICS) as depicted in Fig. 2, both inside-particle and outside-particle have timelike four-momenta, denoted  $p$  and  $k$ , respectively. These particles can interact with each other by “exchange of a virtual photon” if and only if the local energy-momentum conservation law is fulfilled, namely, the condition  $p + k = p' + k'$  must hold (Fig. 1). In addition, the initial particles are arranged to have their closest approach near the event horizon, with the muon inside and the electron outside. An

example of this setup is given in App. A.

The across-horizon Coulomb scattering (AHCS) with these initial momenta and trajectories has a nonvanishing probability in quantum electrodynamics,

$$P_{\text{AHCS}} \Big|_{\text{LICS}} = \left( \left| \begin{array}{c} \text{Diagram of a t-channel scattering process} \\ p' \text{ and } p \text{ are incoming particles, } k' \text{ and } k \text{ are outgoing particles, } q \text{ is the exchanged momentum} \end{array} \right| \right)^2 \begin{array}{l} p+k=p'+k' \\ r(p \text{ wave package}) < r_S \\ r(k \text{ wave package}) > r_S \end{array} > 0, \quad (2)$$

where the standard radial coordinate  $r$  on the right-hand side is expressed in terms of the local inertial coordinates  $\{T, X, Y, Z\}$  (cf. Fig. 2). The probability (2) will be significant if the minimal separation (proper distance  $d$ ) of the two initial particles is of the order of the root of the flat-spacetime cross section (with an infrared cutoff on  $q^2$  determined by the experimental setup).

The initial particles of the scattering reaction (1) are distinguishable: the  $p$  particle has mass  $m_\mu$  and lepton numbers  $(L_e, L_\mu) = (0, 1)$  and the  $k$  particle has mass  $m_e$  and lepton numbers  $(L_e, L_\mu) = (1, 0)$ . Hence, only the  $t$ -channel diagram contributes to (2) and we get the following expression for the flat-spacetime differential cross section in the ultrarelativistic limit ( $E^2 \gg m_\mu^2 \gg m_e^2$ ):

$$\frac{d\sigma}{d\Omega} \Big|_{\text{CM, ultrarel}}^{\text{LICS}} = \frac{\alpha^2}{2 (E_{\text{CM}})^2 (1 - \cos \theta_{\text{CM}})^2} [4 + (1 + \cos \theta_{\text{CM}})^2], \quad (3)$$

with  $E_{\text{CM}}$  and  $\theta_{\text{CM}}$ , respectively, the energy of the initial particles and the scattering angle in the center-of-mass (CM) frame. In fact, expression (3) can also be found as Eq. (5.65) in Ref. [6]. The minimal separation of the two initial particles in (2) must then be as close as possible to

$$d(p \text{ wave package, } k \text{ wave package}) \Big|_{\text{optimal}} \sim \alpha \hbar c / E_{\text{CM}}, \quad (4)$$

where we have used the inequality  $d\sigma/d\Omega \geq \alpha^2/(2E_{\text{CM}}^2)$  from (3) and have temporarily restored  $\hbar$  and  $c$  ( $\alpha \approx 1/137$  is the fine-structure constant). In Fig. 4 of App. A, we have given an example of initial-particle trajectories with a finite value of the minimal separation ( $d_{\text{min}}$ ) between the initial particles. But, in principle, it is also possible to consider head-on collisions.

The result (4) for the optimal proper distance of the two colliding wave packages guarantees having significant scattering, but most scattering will be in the forward direction,  $\theta_{\text{CM}} \sim 0$ . Thus, in the most probable case, the scattered outside-particle disappears behind the Schwarzschild horizon. Still, there is a nonvanishing probability that the outside-particle (electron) recoils due to the Coulomb interaction with the inside-particle (muon). This situation is sketched in Fig. 3 and details are given in Apps. B and C, with an example of

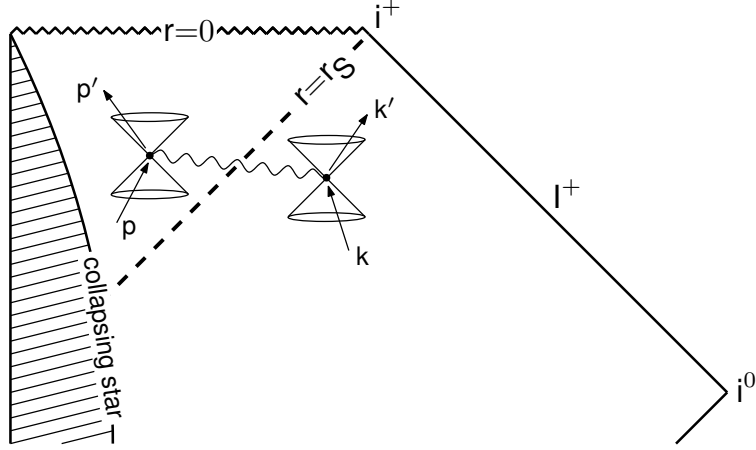


FIG. 3. Part of the Penrose conformal diagram for the Schwarzschild black hole in Kruskal–Szekeres coordinates (the full diagram is shown as Fig. 24 (ii) on p. 154 of Ref. [8], which contains further details). Also shown are two light-cones near the Schwarzschild horizon  $r = r_S$  and the trajectories of two colliding wave packages, one wave package with average momentum  $k$  for the electron is positioned outside the horizon and the other wave package with average momentum  $p$  for the muon is positioned inside the horizon. These particles with momenta  $k$  and  $p$  scatter by virtual-photon exchange (symbolically indicated by the wavy line) and produce, with small but nonvanishing probability, particles with momenta  $k'$  and  $p'$ . The momenta shown correspond to those of the scattering process (1). For ultrarelativistic particles, the momenta are close to their respective light-cones and there is a nonvanishing probability for significant Coulomb scattering if the  $k$  and  $p$  wave packages approach each other within a proper distance of order  $\alpha \hbar c/E_{\text{CM}}$ , where  $E_{\text{CM}}$  is the center-of-mass energy in the local inertial coordinate system and  $\alpha$  the fine-structure constant.

final-particle trajectories given in Fig. 5. The ultrarelativistic recoil electron  $k'$  in Fig. 3 crosses the constant- $r$  curves in the Penrose diagram (cf. Fig. 24 (ii) in Ref. [8]) and moves away from the black-hole horizon. There is, then, a nonvanishing probability that the  $k'$  electron triggers an outside-region detector far away from the interaction point. This last observation is an essential ingredient of the *Gedankenexperiment* to be discussed next.

### III. GEDANKENEXPERIMENT

The setup of our *Gedankenexperiment* is as follows:

1. a large-mass nonrotating black hole with static Schwarzschild metric;
2. two quasi-stationary experimenters, Castor and Pollux, who perform their experiments rapidly enough, so that their positions with respect to the Schwarzschild horizon do not change substantially;

3. Castor and Pollux use the scattering process from Sec. II and Fig. 3 with pre-determined initial momenta  $p$  and  $k$ , which are arranged to give, with largest possible probability, a nontrivial scattering event with recoil momentum  $k'$ ;
4. Castor and Pollux meet in the exterior region and agree on the following procedure:
  - 4a. along a fixed radial direction, Castor rapidly moves inside the Schwarzschild horizon, while Pollux stays outside;
  - 4b. at a pre-arranged moment, Pollux starts to emit, at regular time intervals, appropriate electrons [each of momentum  $k$  from (1) and App. A] and sends out  $N$  electrons in total;
  - 4c. starting from the corresponding pre-arranged moment and at an appropriately adjusted rate, Castor either emits  $N$  appropriate muons [each of momentum  $p$  from (1) and App. A] or sends no such muons at all; in the first case, Castor writes in his message-book a “yes” and, in the second case, he writes a “no”;
  - 4d. if Castor has emitted  $N$  muons  $p$ , then Pollux’s detector (positioned at an appropriate distance away from the black-hole horizon) has a nonzero chance to register a momentum change of the exterior electron as discussed in Apps. B and C [Pollux writes “1” in his log-book if he does register a recoil electron with momentum  $k' \neq k$  and “0” if he does not register a recoil electron], but if Castor has emitted no muons  $p$ , then Pollux’s detector will never register a recoil electron [Pollux writes  $N$  times a “0” in his logbook];
  - 4e. after  $N$  measurements, Pollux looks at his logbook and summarizes his results as follows: a sequence of  $N$  zeros is written as “NO” and a sequence with at least a single “1” is written as “YES”;
5. according to points 4c and 4e, Castor can send a message (“yes” or “no” in his message-book), which is read by Pollux (“YES” or “NO” in his logbook);
6. as Castor’s message-book is in the interior region of the Schwarzschild black-hole horizon and Pollux’s log-book in the exterior region, information (“yes” or “no”) has been transferred outwards, across the Schwarzschild black-hole horizon;
7. Pollux can transmit the message in his logbook (“YES” or “NO”) to distant observers by classical means; see Sec. IV for further discussion.

A few technical remarks are in order:

ad 4b. Castor and Pollux’s procedure can be extended by having several sequences (labeled  $i = 1, \dots, I$ ) with each  $N_i^P = N$  electrons emitted by Pollux and  $N_i^C = N/0$  muons emitted by Castor, so that Castor’s whole message is (yes/no, yes/no,  $\dots$ , yes/no) with  $I$  entries.

ad 4d. As the probability for getting a measurable kick of the exterior electron is small (see Apps. B and C),  $N$  needs to be taken sufficiently large.

ad 4e. It is possible that Pollux's detector records a false “1”, so that the read message is not error-free and the criterium for Pollux to write a “YES” in his logbook may need to be sharpened (with a corresponding change for the “NO” criterium). Castor and Pollux may also decide to use an error-correcting code for the  $I$ -entries message mentioned in the first technical remark.

All these technical issues are engineering questions and need to be addressed. Note that the whole experimental setup of Castor and Pollux (with a muon factory, a linear accelerator for muons, an electron source, a linear accelerator for electrons, and a detector for electrons) has a substantial mass, but still very much less than the black-hole mass  $M$  which can be made arbitrarily large (at least, in a *Gedankenexperiment*).

#### IV. DISCUSSION

Heuristically, across-horizon Coulomb scattering appears to be quite natural. Assume that a nonrotating astrophysical black hole is initially neutral and that, at a later moment, a particle of electric charge  $Q$  falls in, crossing the Schwarzschild horizon. From a macroscopic point of view, this charged particle changes the Schwarzschild black hole into a Reissner–Nordstrøm black hole of charge  $Q$ . In other words, although the charged particle was “swallowed” by the black hole, its charge  $Q$  has not disappeared for the region outside the black-hole horizon and can still influence the outside-charges. From a microscopic point of view, this Coulomb interaction happens due to virtual-photon exchange.

Referring to the Schwarzschild black-hole horizon, the momentum exchange  $q$  between inside-particles and outside-particles is a measurable observable (Sec. II and App. C). An outside-observer can measure, in principle, the corresponding momentum change of the outside-electron, but not the charge of the inside-particle or its initial momentum. It appears that the across-horizon-Coulomb-scattering effect can be employed to encode a message, which can be sent by an inside-observer to an outside-observer (Sec. III).

It is sometimes said that “an event horizon is the boundary in spacetime between events that can communicate with distant observers and events that cannot” (quote from Sec. 11.3, 2nd paragraph in Ref. [9]). In view of the results of the present article, this statement needs to be refined (it still being understood that the spacetime manifold is a classical concept): “an event horizon is the boundary in spacetime between events that can communicate with distant observers by classical means and events that cannot.” Nature is, of course, not classical ( $\hbar \neq 0$ ) and this fact allows for a potential breach of the event horizon as defined by the second statement. We have indeed shown that quantum scattering allows, in principle, for the transfer of information from inside the event horizon to outside.

In this article, we have focussed on across-horizon Coulomb scattering for astrophysical black holes, but similar effects may occur in analogue systems [10, 11].

## Appendix A: Initial-particle trajectories

In this appendix, we give an example of initial-particle trajectories which have their closest approach near the Schwarzschild black-hole horizon, with one particle (muon) inside and the other particle (electron) outside. Both particles are considered to be ultrarelativistic and  $c$  is set to unity. But, before we discuss these initial-particle trajectories, we have a remark on the meaning of the event horizon.

Generally speaking, the event horizon is a global notion in the sense that it depends on the observer's entire geodesic history and the large-scale structure of spacetime [8]. The black-hole event horizon, in particular, is associated with a null hypersurface which corresponds to the boundary between null rays that cannot come out and those that can. This horizon surface can be projected locally on the local inertial coordinate system (LICS) of the near-horizon region. By the Einstein equivalence principle, the physics in the LICS is the same as that of flat Minkowski spacetime and nothing distinguishes locally the projected horizon surface, only that part of this surface coincides with part of the light-cone.

With appropriate local inertial coordinates  $\{T, X, Y, Z\}$  near the Schwarzschild horizon (Fig. 2) and a very large black-hole mass  $M$ , the horizon coincides with a disk-like patch of the  $(Y, Z)$ -plane centered around  $(Y, Z) = (0, 0)$  and at position

$$X_{\text{hor}} = T. \quad (\text{A1})$$

For the initial wave packages, we can take the following trajectories:

$$(X, Y, Z)_{e, \text{in}} \sim \left( -\sqrt{1/3} T + d_0 - d_\mu, \sqrt{2/3} T, 0 \right), \quad (\text{A2a})$$

$$(X, Y, Z)_{\mu, \text{in}} \sim (T - d_\mu, 0, 0), \quad (\text{A2b})$$

where the nonzero particle masses have been neglected for the velocities. The distance between the two wave packages is given by

$$d(T) = \sqrt{(X_\mu - X_e)^2 + (Y_\mu - Y_e)^2 + (Z_\mu - Z_e)^2}, \quad (\text{A3})$$

and the trajectories (A2) result in having  $d(0) = d_0$ .

An example of these trajectories is given in Fig. 4, where, at the moment of closest approach ( $T = 1$ ), the electron is still outside the horizon,  $X_{e, \text{in}}(1) > X_{\text{hor}}(1)$ , while the muon is always inside,  $X_{\mu, \text{in}}(T) < X_{\text{hor}}(T)$ . Dispersion and scattering effects are neglected. The particular initial-particle trajectories of Fig. 4 for a length scale of the order of (4) give the momentum  $k$  for the electron and the momentum  $p$  for the muon, which enter the amplitude (1).

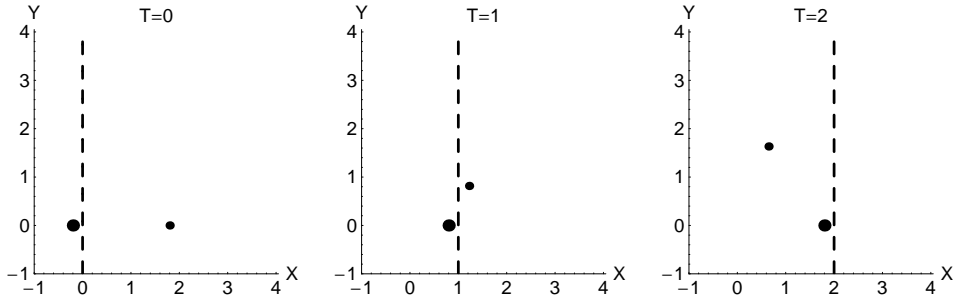


FIG. 4. Initial wave-package trajectories in the  $(X, Y)$ -plane from (A2a) and (A2b), without dispersion and scattering. The muon wave package (large dot) has increasing values of  $X$  and a constant value of  $Y$ . The electron wave package (small dot) has decreasing values of  $X$  and increasing values of  $Y$ . The black-hole horizon from (A1) is shown as the dashed line. With an arbitrary length unit, the parameters in (A2) are chosen as  $\{d_0, d_\mu\} = \{2, 1/5\}$ . The minimum separation  $d_{\min} \approx 0.92$  occurs at  $T_{\min} = 1$ . For a length scale of the order of (4), significant Coulomb scattering occurs, as discussed in Sec. III and App. C.

Remark that, if the muon initially has a velocity with nonzero  $Y$  and  $Z$  components, the horizon at position (A1) runs away from that particle and the situation sketched in the middle panel of Fig. 4 does not occur. The coordinate  $X$  lies, to leading order, in the radial direction of the black-hole spacetime (Fig. 2). The conclusion is, thus, that the initial ultrarelativistic muon (momentum  $p$  in Fig. 3) must have, to high precision, an outward radial motion.

## Appendix B: Final-particle trajectories

In this appendix, we give a simplified discussion of how Coulomb scattering may affect the motion of the initial particles. In App. C, we give a detailed calculation of the quantum scattering process in position space.

For the initial trajectories of App. A, the large-angle Coulomb scattering probability is significant if the minimal distance in Fig. 4 is of order  $\alpha \hbar c / E_{\text{CM}}$ , based on the estimate (4) in terms of the center-of-mass scattering energy  $E_{\text{CM}}$ . In that case, there is a nonvanishing probability that the electron recoils. An example of such a recoil trajectory is as follows:

$$(X, Y, Z)_{e, \text{out}} \Big|^{(T>1)} \sim (X_{e, \text{out}, 1} + \sqrt{1/2} (T - 1), Y_{e, \text{out}, 1} + \sqrt{1/2} (T - 1), 0), \quad (\text{B1})$$

with a matching muon trajectory from energy-momentum conservation. The constants  $(X_{e, \text{out}, 1}, Y_{e, \text{out}, 1})$  in (B1) correspond approximately to the position of the initial electron at  $T = 1$  in Fig. 4. A recoil electron with trajectory (B1) is, however, rapidly overrun by the horizon at position (A1). Remark that, for a genuine scattering process, we should only

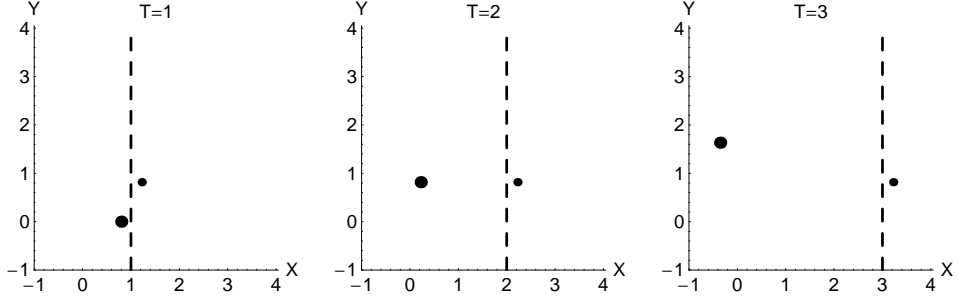


FIG. 5. Final wave-package trajectories in the  $(X, Y)$ -plane from (B2a) and (B2b), with Coulomb scattering taking place at  $T \sim 1$ . The constants  $(X_{e, \text{out}, 1}, Y_{e, \text{out}, 1})$  and  $(X_{\mu, \text{out}, 1}, Y_{\mu, \text{out}, 1})$  have been taken equal to the  $T = 1$  positions of the initial-particle trajectories (A2a) and (A2b), as shown in Fig. 4 for  $T \leq 1$  and a length scale of the order of (4).

consider the electron in (B1) at  $T \gg 1$ , but we have simplified the discussion somewhat by taking  $T > 1$ .

Consider, next, a different trajectory of the recoil electron,

$$(X, Y, Z)_{e, \text{out}} \Big|^{(T>1)} \sim (X_{e, \text{out}, 1} + (T - 1), Y_{e, \text{out}, 1}, 0), \quad (\text{B2a})$$

$$(X, Y, Z)_{\mu, \text{out}} \Big|^{(T>1)} \sim (X_{\mu, \text{out}, 1} - \sqrt{1/3} (T - 1), Y_{\mu, \text{out}, 1} + \sqrt{2/3} (T - 1), 0), \quad (\text{B2b})$$

with constants  $(X_{e, \text{out}, 1}, Y_{e, \text{out}, 1})$  and  $(X_{\mu, \text{out}, 1}, Y_{\mu, \text{out}, 1})$  corresponding approximately to the positions of the initial particles at  $T = 1$  in Fig. 4. Now, the final electron has a velocity purely in the  $X$  direction and the final electron stays outside the horizon, provided  $X_{e, \text{out}, 1} > 1$ . Figure 5 shows these final trajectories. The particular final-particle trajectories of Fig. 5 for a length scale of the order of (4) give the momentum  $k'$  for the electron and the momentum  $p'$  for the muon, which enter the amplitude (1).

The final recoil electron of (B2a) is special in that its  $Y$  and  $Z$  velocity components are exactly zero. Let us estimate which changes in that velocity direction are allowed if we demand that the final ultrarelativistic recoil electron stays outside the black-hole horizon, at least, over the Minkowski patch considered.

The curvature scale is given by  $r_S = 2 G_N M/c^2$  and the Minkowski patch has approximately that size. If we now assume that, just after the scattering moment  $T \sim 1$ , the recoil electron is outside the horizon by a distance  $\tilde{d} \sim X_{e, \text{out}, 1} - 1 \sim \alpha \hbar c/E_{\text{CM}}$  in the  $X$  direction, then we find that the electron trajectory can differ from the trajectory (B2a) by a small angle  $\delta$  which is of order

$$\delta \sim \sqrt{2 \tilde{d}/r_S} \sim \sqrt{\alpha} E_P / \sqrt{E_{\text{CM}} M c^2}, \quad (\text{B3})$$

with Planck energy  $E_P \equiv \sqrt{\hbar c^5/G_N} \approx 1.22 \times 10^{19} \text{ GeV} \approx 2.18 \times 10^{-5} \text{ g}$ . The conclusion is that the allowed solid angle  $\delta^2$  of the recoil electron (momentum  $k'$  in Fig. 3) is extremely

small:  $\delta^2 \sim 10^{-36}$  for  $E_{\text{CM}} \sim 10^{15} \text{ GeV}$  and  $M \sim M_{\text{Sun}} \sim 10^{38} E_P$ .

A related issue is that the recoil electron must have a sufficiently large energy [a large enough gamma factor  $E(k')/(m_e c^2)$ ], so that the electron is not overrun by the horizon (A1) before the electron reaches the edge of the Minkowski patch at  $X \sim r_S$ . Taking that the recoil electron at  $T \sim 1$  is outside the horizon by a distance  $\tilde{d} \sim \alpha \hbar c / E_{\text{CM}}$  in the  $X$  direction, and assuming a velocity purely in the  $X$  direction and an energy of order  $E_{\text{CM}}/2$ , we get the following estimate for the required center-of-mass scattering energy:

$$E_{\text{CM}} \gtrsim 4 \frac{1}{\alpha} \frac{m_e c^2}{E_P} \frac{M c^2}{E_P} m_e c^2, \quad (\text{B4})$$

where  $m_e \approx 0.511 \text{ MeV}/c^2$  is the electron mass and  $M$  the black-hole mass. With  $M \sim M_{\text{Sun}}$ , the required scattering energy is  $E_{\text{CM}} \gtrsim 10^{15} \text{ GeV}$ , which is large but still less than the Planck energy  $E_P$ .

### Appendix C: Probability amplitude in position space

In this appendix, we discuss the scattering process (1) in position space and refer to, e.g., Ref. [6] for further details and notation.

Consider the following Hilbert-space state:

$$|\chi^s(X, k)\rangle = \int \frac{d^3\mathbf{K}}{(2\pi)^3} \frac{1}{2E_{\mathbf{K}}} e^{iKX} \bar{u}^s(K) \varphi_k(K) |\mathbf{K}, s\rangle, \quad (\text{C1})$$

with the conjugate 4-spinor  $\bar{u}_\alpha^s(K)$  from the plane-wave solution of the conjugated Dirac equation and the further definitions  $k^0 \equiv E_{\mathbf{k}} = (\mathbf{k}^2 + m^2)^{1/2}$ ,  $K^0 \equiv E_{\mathbf{K}} = (\mathbf{K}^2 + m^2)^{1/2}$ , and

$$\varphi_k(K) \equiv N \exp\left(-\frac{(\mathbf{K} - \mathbf{k})^2}{4\sigma^2}\right), \quad (\text{C2})$$

for normalization factor  $N$  and momentum variance  $\sigma$ . The ket  $|\chi^s(X, k)\rangle$  corresponds to a one-particle state of spin  $s = \pm 1/2$ , which is localized in position space around  $X$  and in momentum space around  $k$ . Here,  $X$  is a short-hand notation of the local inertial coordinates  $\{T, X, Y, Z\}$  used in Apps. A and B. Similarly,  $k$  is a short-hand notation for the corresponding 4-momentum.

Suppose that the free initial particle is described by  $|\chi^s(X, k)\rangle$ . The probability amplitude  $A_{k \rightarrow k}(X'|X)$  for detecting this particle at  $X'$  is then given by the following projection:

$$A_{k \rightarrow k}^{(s; s)}(X'|X) \equiv \langle \chi^s(X', k) | \chi^s(X, k) \rangle \quad (\text{C3})$$

$$= \int \frac{d^3\mathbf{K}}{(2\pi)^3} \frac{1}{2E_{\mathbf{K}}} e^{iK(X-X')} |\varphi_k(K)|^2 (\bar{u}^s(K) u^s(K)).$$

It is straightforward to show numerically that  $|A_{k \rightarrow k}^{(s; s)}(X'|X)|^2$  has a maximal value if the wave package moves along the classical trajectory,  $\mathbf{X}' = \mathbf{X} + (\mathbf{k}/E_{\mathbf{k}})(T' - T)$ .

Suppose, now, that we have two particles (electron and muon) at past infinity, which are initially far away from each other and are described by  $|\chi^r(\tilde{X}, p)\rangle$  and  $|\chi^s(X, k)\rangle$ , respectively. If these two particles do not interact with each other, then we find the following probability amplitude:

$$\begin{aligned} A_{p,k \rightarrow p,k}^{(r,s; r,s)}(\tilde{X}'; X' | \tilde{X}; X) \Big|_{\text{free}} &\equiv \langle \chi^r(\tilde{X}', p); \chi^s(X', k) | \chi^r(\tilde{X}, p); \chi^s(X, k) \rangle \\ &= A_{p \rightarrow p}^{(r,r)}(\tilde{X}' | \tilde{X}) A_{k \rightarrow k}^{(s,s)}(X' | X). \end{aligned} \quad (\text{C4})$$

If the two particles (electron and muon) interact with each other via the electromagnetic field, we obtain at tree-level

$$\begin{aligned} &A_{p,k \rightarrow p',k'}^{(r,s; r',s')}(\tilde{X}'; X' | \tilde{X}; X) \Big|_{\text{tree}} \equiv \langle \chi^{r'}(\tilde{X}', p'); \chi^{s'}(X', k') | \chi^r(\tilde{X}, p); \chi^s(X, k) \rangle \\ &= \int \frac{d^3 \mathbf{K}'}{(2\pi)^3} \frac{d^3 \mathbf{K}}{(2\pi)^3} \frac{d^3 \mathbf{P}'}{(2\pi)^3} \frac{d^3 \mathbf{P}}{(2\pi)^3} \frac{1}{16 E_{\mathbf{K}} E_{\mathbf{K}'} \mathcal{E}_{\mathbf{P}} \mathcal{E}_{\mathbf{P}'}} e^{iKX - iK'X' + iP\tilde{X} - iP'\tilde{X}'} \\ &\times (\bar{u}^r(P) u^{r'}(P')) (\bar{u}^s(K) u^{s'}(K')) (\varphi_{p'}^*(P') \varphi_p(P)) (\varphi_{k'}^*(K') \varphi_k(K)) \\ &\times \langle_{\text{out}} \langle \mathbf{P}', r'; \mathbf{K}', s' | \mathbf{P}, r; \mathbf{K}, s \rangle_{\text{in}}, \end{aligned} \quad (\text{C5a})$$

with definitions  $K^0 \equiv E_{\mathbf{K}} = (\mathbf{K}^2 + m_e^2)^{1/2}$  and  $P^0 \equiv \mathcal{E}_{\mathbf{P}} = (\mathbf{P}^2 + m_{\mu}^2)^{1/2}$ , and the general expressions

$$\langle_{\text{out}} \langle p', r'; k', s' | p, r; k, s \rangle_{\text{in}} = (2\pi)^4 \delta^4(p' + k' - p - k) i\mathcal{M}_{r,r'}^{s,s'}(p, k \rightarrow p', k'), \quad (\text{C5b})$$

$$i\mathcal{M}_{r,r'}^{s,s'}(p, k \rightarrow p', k') = \frac{ie^2}{q^2 + i\epsilon} \bar{u}^{r'}(p') \gamma^\mu u^r(p) \bar{u}^{s'}(k') \gamma_\mu u^s(k), \quad (\text{C5c})$$

where lower-case symbols  $p$ ,  $k$ ,  $p'$ , and  $k'$  denote off-shell 4-momenta, the momentum exchange  $q$  is given by  $p' - p$ , and  $\epsilon$  is the positive infinitesimal of the Feynman photon propagator. Recall that  $|\mathcal{M}|^2$  (averaged and summed over spins) is the main ingredient of the differential cross section (3).

The total perturbative 2-2 Coulomb scattering amplitude is given by the sum of the free contribution [of order  $e^0$ ], the tree-level contribution [of order  $e^2$ ], and the renormalized  $n$ -loop contributions [each of order  $e^{2(n+1)}$  for  $n \geq 1$ ].

With the initial and final trajectories of the electron and muon from Figs. 4 and 5 for a length scale of the order of (4), we obtain numerically that the corresponding probability  $|A_{p,k \rightarrow p',k'}^{(r,s; r',s')}(\tilde{X}'; X' | \tilde{X}; X)|^2$  is nonvanishing at tree-level, which gives the recoil electron needed for the *Gedankenexperiment* of Sec. III.

---

- [1] S.W. Hawking, “Particle creation by black holes,” *Commun. Math. Phys.* **43**, 199 (1975), Erratum: *Commun. Math. Phys.* **46**, 206 (1976).
- [2] W.G. Unruh and R.M. Wald, “Information loss,” *Rept. Prog. Phys.* **80**, 092002 (2017), arXiv:1703.02140.
- [3] V.A. Emelyanov, “QED loop effects in the spacetime background of a Schwarzschild black hole,” arXiv:1710.01049.
- [4] R.P. Feynman, “Space-time approach to quantum electrodynamics,” *Phys. Rev.* **76**, 769 (1949).
- [5] M.J.G. Veltman, *Diagrammatica: The Path to Feynman Rules* (Cambridge University Press, 1994).
- [6] M.E. Peskin and D.V. Schroeder, *An Introduction to Quantum Field Theory* (Addison-Wesley Publishing Co., 1995).
- [7] R. Gautreau, “Light cones inside the Schwarzschild radius,” *Am. J. Phys.* **63**, 431 (1995).
- [8] S.W. Hawking and G.F.R. Ellis, *The Large Scale Structure of Space-Time* (Cambridge University Press, Cambridge, England, 1973).
- [9] B.F. Schutz, *A First Course in General Relativity*, Second Edition (Cambridge University Press, Cambridge, England, 2009).
- [10] S. Weinfurtner, E.W. Tedford, M.C.J. Penrice, W.G. Unruh, and G.A. Lawrence, “Measurement of stimulated Hawking emission in an analogue system,” *Phys. Rev. Lett.* **106**, 021302 (2011), arXiv:1008.1911.
- [11] L.-P. Euvé, F. Michel, R. Parentani, T.G. Philbin, and G. Rousseaux, “Observation of noise correlated by the Hawking effect in a water tank,” *Phys. Rev. Lett.* **117**, 121301 (2016), arXiv:1511.08145.